

# A Low-Current Pulsed Electric Field Treatment System for Fruit Juices: Air-Gap Optimisation and Assessment of Microbial Inactivation

Thomas Mohan<sup>1,2,\*</sup>, Aswini S. Choolangal<sup>3</sup>, Noorul H. M. Noor<sup>4</sup>, Krishnan J. Suja<sup>1</sup>,  
Karakkat M. Sunitha<sup>4</sup>, and Tharamel V. Suchithra<sup>3</sup>

<sup>1</sup>Department of Electronics & Communication Engineering, National Institute of Technology Calicut, India

<sup>2</sup>Department of Electronics & Communication Engineering, Mar Athanasius College of Engineering, Kerala, India

<sup>3</sup>Department of Bioscience and Engineering, National Institute of Technology Calicut, India

<sup>4</sup>Department of Electrical Engineering, National Institute of Technology Calicut, India

**ABSTRACT:** The use of electromagnetic fields to inactivate microorganisms and preserve food items is gaining increasing popularity. Among the different electromagnetic treatments used for fruit juice preservation, Pulsed Electric Field (PEF) treatment is a prominent method. However, in the Pulsed Electric Field treatment chambers currently used, the current flow and energy dissipation within the juice are very high. These high currents cause unwanted electrochemical reactions inside the juice, increasing its temperature. This work introduces a method to prevent it by reducing the current flow with the help of an air gap inside the Pulsed Electric Field treatment chamber. A mathematical model of the proposed system was created, and the reduced current values were calculated. Simulations using COMSOL Multiphysics software were conducted to analyze the electric field distribution and the increase in juice temperature. The optimum value of the air gap that can be provided inside the chamber without the risk of electrical breakdown was determined through simulations of the electric field intensities and later confirmed through experiments. The effectiveness of the proposed system in inactivating microbes was assessed through microbiological experiments using *Escherichia coli* in watermelon juice. According to the experimental results, the proposed system successfully achieved bacterial inactivation with a low current value and without any measurable increase in the juice temperature. To the best of our knowledge, there are very limited studies addressing the reduction of current flow within a Pulsed Electric Field treatment chamber through the incorporation of air gaps. In the future, this novel method for preserving fruit juices could be highly beneficial to the food processing industry.

## 1. INTRODUCTION

Pulsed Electric Field (PEF) treatment is an emerging electromagnetic field-based technique for food preservation. In PEF treatment systems, food items, such as fruit juices, are exposed to a uniform distribution of high-intensity electric fields to extend their shelf life. Compared to conventional thermal treatment, PEF treatment is better at preserving aroma, color [1, 2], and nutritional components, such as Vitamin C and polyphenols [3–5]. During PEF treatment, high-voltage pulses cause irreversible electroporation in the cell membranes of microorganisms, which kills them [6, 7]. Typically, electric fields of the order of tens of kV/cm are applied to fruit juices during PEF treatment [1, 4, 8]. The existing PEF treatment techniques also have certain drawbacks. Because fruit juices are highly conductive, the application of such high electric fields creates hundreds [9, 10] or even thousands [6, 11] of amperes of current through the juice. Such a high current flow causes electrochemical reactions at the electrode-juice interface, which releases small quantities of metal ions and other harmful chemicals [11, 12] into the juice.

A high current flow also increases the juice temperature. Previously published results [3, 4, 13] indicate an increase in juice temperature of nearly 20°C after PEF treatment. This local heating causes partial evaporation of the water in the juice, creating gas bubbles that can trigger undesirable electrical breakdown within the treatment chambers [14, 15]. A large temperature rise also affects the freshness [16] and physical properties of food materials [17]. Additional cooling mechanisms installed in the PEF treatment chamber to control the temperature [18, 19] increase the setup cost. Furthermore, to supply hundreds of amperes of current through the juice, expensive PEF signal generators with high current ratings are required. For these reasons, it is desirable to have a smaller current flow through the juice during PEF treatment.

The objective of this study was to design a PEF treatment system with lower current flow through the juice. The current was reduced by introducing an air gap below the top electrode in the parallel-plate electrode system. Owing to the high impedance of the air gap, only a small amount of current flows through the chamber. One drawback of this method is that the air gap results in a lower electric field intensity across the juice. Timmermans et al. [20] achieved successful microbial inactivation

\* Corresponding author: Thomas Mohan (thomas.mohan@mace.ac.in).

by providing lower electric field strengths for longer durations. Similarly, in this study, the reduction in the electric field due to the air gap was compensated for by increasing the number of pulses used for treatment.

Watermelon juice contains high quantities of spoilage microorganisms and has a short shelf life [21]. Under normal refrigeration conditions, fresh watermelon juice is reported to have a shelf life of only 4 hours [22, 23]. Compared to other juices, such as orange and apple juices, there are fewer studies on PEF treatment of watermelon juice. Therefore, watermelon juice was used to test the proposed system. First, the current flow through the chamber is calculated using a mathematical model. Finite Element Analysis using COMSOL Multiphysics software has been successfully employed for thermal analysis in various studies [24]; therefore, it was utilized in our study to calculate the temperature rise within the juice. An electric field analysis using COMSOL was employed to determine the optimal height of the air gap that dissipated the maximum power inside the juice without causing electrical breakdown, which was subsequently validated through experiments. Finally, the effectiveness of the proposed treatment chamber in inactivating microbes was assessed using microbiological experiments.

Most existing studies on PEF treatment have reported high current flow and an unwanted increase in juice temperature. The air gap in our study enabled low-current juice processing without a significant increase in temperature. While some studies have investigated the usage of ceramic-coated electrodes [6, 10, 25] to reduce the current flow, this work introduces a novel method for PEF treatment chambers with air gaps. The physical implementation, field distribution characteristics, breakdown constraints, and system-level implications of the proposed air-gap configuration differ fundamentally from those of ceramic-coated electrode systems. Watermelon juice was used for experimental validation in our study. In the future, this study could be further improved and extended to the treatment of other fruit juices.

## 2. MATERIALS AND METHODS

### 2.1. Mathematical Modelling

#### 2.1.1. Voltages and Currents inside the Chamber

In the proposed system, a high-voltage double exponential voltage pulse with an amplitude of 20 kV, rise time of 1.2  $\mu$ s, and pulse width of 50  $\mu$ s (full width half maximum value) was used. The general equation for a double exponential signal is given by

$$v(t) = V_0 k (e^{-\alpha t} - e^{-\beta t}) \quad (1)$$

where  $V_0$  is the amplitude;  $\alpha$  and  $\beta$  are characteristic mathematical parameters; and  $k$  is the amplitude factor. Based on the required specifications of the pulse, the parameters were calculated as  $\alpha = 14868.04$ ,  $\beta = 1629782.1$ , and  $k = 1.05$  using the equations described by Magdowski and Vick [26].

The proposed treatment chamber contains a layer of air below the top electrode. This air gap acts as a capacitor, whose high impedance lowers the current through the chamber. Fig. 1

shows the equivalent electrical model of the chamber. The watermelon juice inside the chamber was modelled as a parallel combination of a resistor ( $R_{juice}$ ) and capacitor ( $C_{juice}$ ).

For a cylindrical column of juice with depth  $l$  and area of cross section  $A$ , the resistance and reactance are calculated as follows:

$$R_{juice} = l/\sigma A \quad (2)$$

$$X_{juice} = l/(2\pi f \varepsilon_0 \varepsilon_r A) \quad (3)$$

where  $\sigma$  is the juice conductivity;  $f$  is the applied signal frequency;  $\varepsilon_0$  is the absolute permittivity of free space; and  $\varepsilon_r$  is the relative permittivity of the watermelon juice. For  $\sigma = 2.3$  mS/cm,  $\varepsilon_r = 95$  [27], and  $f = 10$  kHz (center frequency of a pulse of width 50  $\mu$ s), the ratio of  $X_{juice} : R_{juice} = 4352 : 1$ . Because  $X_{juice} \gg R_{juice}$ ,  $X_{juice}$  is ignored in the parallel combination, and the juice is modelled with resistor  $R = R_{juice}$ . This assumption works well for frequencies in the range of kHz, though at much higher frequencies in the order of MHz, it can lead to errors in the final computed values. From the simplified equivalent circuit, the applied voltage can be expressed as follows:

$$v(t) = v_C(t) + Ri(t) \quad (4)$$

where  $v_C(t)$  is the voltage across the air gap, and  $i(t)$  is the chamber current. Using Eq. (1) in Eq. (4) and rearranging, we obtain the following linear differential equation:

$$\frac{dv_C}{dt} + \frac{v_C}{RC} = \frac{V_0 k}{RC} (e^{-\alpha t} - e^{-\beta t}) \quad (5)$$

By solving this linear differential equation and applying the initial value condition that  $v_C = 0$  at  $t = 0$ , the expression for  $v_C$  is obtained as

$$v_C = \frac{V_0 k}{RC} \left[ \frac{e^{-\alpha t}}{\frac{1}{RC} - \alpha} - \frac{e^{-\beta t}}{\frac{1}{RC} - \beta} \right] - \frac{V_0 k}{RC} \left[ \frac{e^{-t/RC}}{\frac{1}{RC} - \alpha} - \frac{e^{-t/RC}}{\frac{1}{RC} - \beta} \right] \quad (6)$$

From Eq. (6), the current flowing through the chamber is obtained, as shown in Eq. (7).

$$i(t) = \frac{V_0 k}{R} \left[ \frac{\frac{1}{RC} e^{-t/RC} - \alpha e^{-\alpha t}}{\frac{1}{RC} - \alpha} \right] - \frac{V_0 k}{R} \left[ \frac{\frac{1}{RC} e^{-t/RC} - \beta e^{-\beta t}}{\frac{1}{RC} - \beta} \right] \quad (7)$$

As the thickness of the air gap increased, the current decreased, and the energy dissipation within the juice decreased. Hence, smaller air gaps result in higher levels of microbial inactivation. Air gaps ranging from 1.0 cm to 4.5 cm were considered for the analysis. Air gaps thinner than 1.0 cm were excluded, as they may be susceptible to electrical breakdown. This assumption was experimentally validated. To analyze the significance of the air gap in limiting the current, scenarios with and without an air gap were compared.

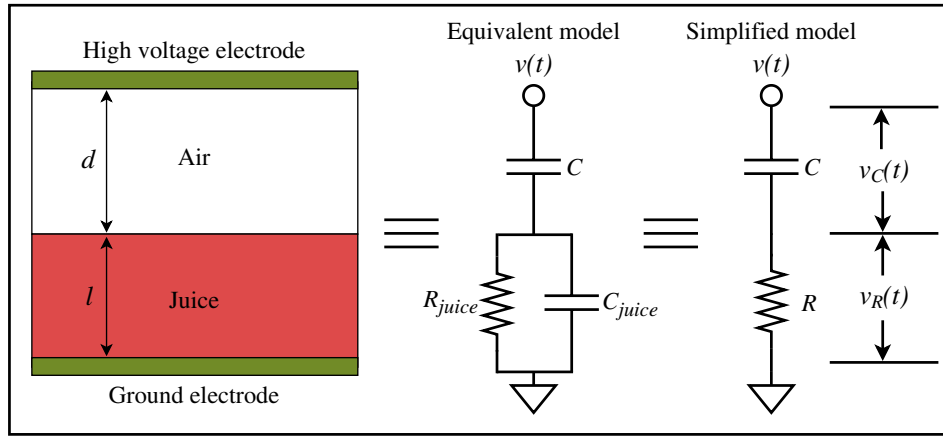


**FIGURE 1.** Electrical equivalent model of the proposed treatment chamber. Capacitance  $C$  represents the air gap above the juice.

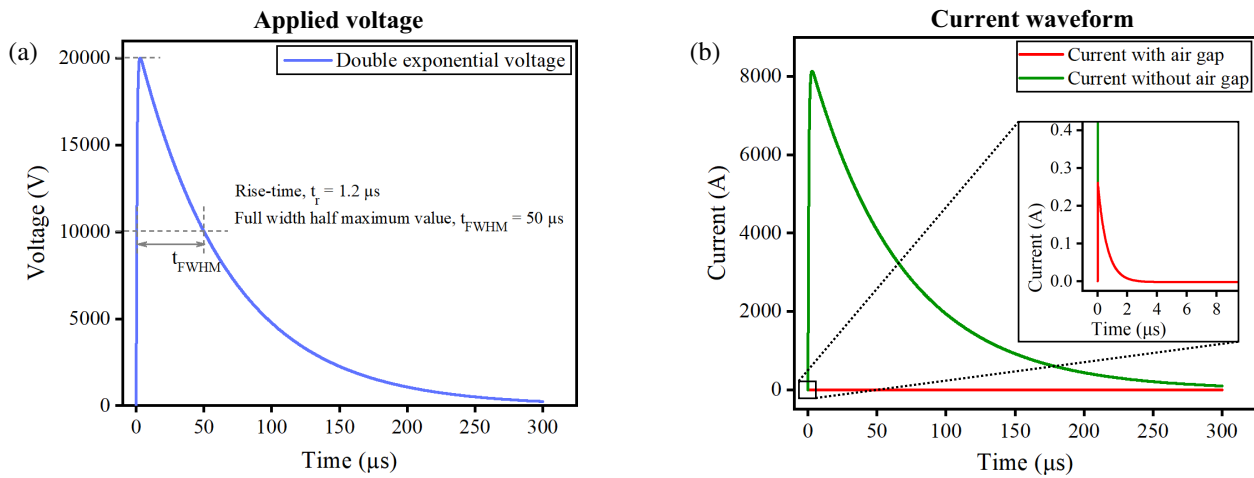


**FIGURE 2.** (a) Applied double exponential voltage (b) Current through juice — with air gap (2 cm) and without air gap. Inset contains a selected portion of the graph for time  $t$  up to 10  $\mu\text{s}$ .

**2.1.2. Comparison with Currents in the Absence of Air Gaps**

A chamber without an air gap was modelled with resistor  $R$  (resistance of the juice) across the applied voltage. Here, the current is given by:

$$i(t) = \frac{V_0 k}{R} (e^{-\alpha t} - e^{-\beta t}) \quad (8)$$

A comparison of the plots of currents without an air gap and with an air gap (2.0 cm) obtained using Eq. (7) and Eq. (8) is shown in Fig. 2. With an air gap, the peak current was found to be low, and the spike was very narrow. Therefore, power dissipation occurred only for a short duration, thus limiting the increase in juice temperature.

**2.2. Finite Element Analysis**

Simulations using COMSOL Multiphysics software had two objectives. The first was to analyze the temperature increase inside the juice, and the second was to determine the thickness of the air gap at which undesirable electrical breakdown

occurred. The simulation results were subsequently validated through experiments.

**2.2.1. Simulation of the Rise in Juice Temperature**

The *Electric Currents*, *Heat Transfer*, and *Electromagnetic Heating* modules in COMSOL were used for the simulation. The *Electric Currents* module used Eq. (9) to calculate the total current density,  $\mathbf{J}$ .

$$\mathbf{J} = \sigma \mathbf{E} + \partial \mathbf{D} / \partial t + \mathbf{J}_e \quad (9)$$

where  $\sigma$  is the conductivity of the medium;  $\mathbf{E}$  is the electric field intensity;  $\partial \mathbf{D} / \partial t$  is the displacement current density; and  $\mathbf{J}_e$  is the externally generated current density. The electric field intensity was calculated using the following equation:

$$\mathbf{E} = -\nabla V \quad (10)$$

where  $\nabla V$  is the electric potential gradient. The *Heat Transfer* module solved the transient bioheat equation [28] given by Eqs. (11) and (12) to calculate the associated variables.

$$\rho C_p \partial T / \partial t + \rho C_p \mathbf{u} \cdot \nabla T + \nabla \cdot \mathbf{q} = Q + Q_{ted} \quad (11)$$

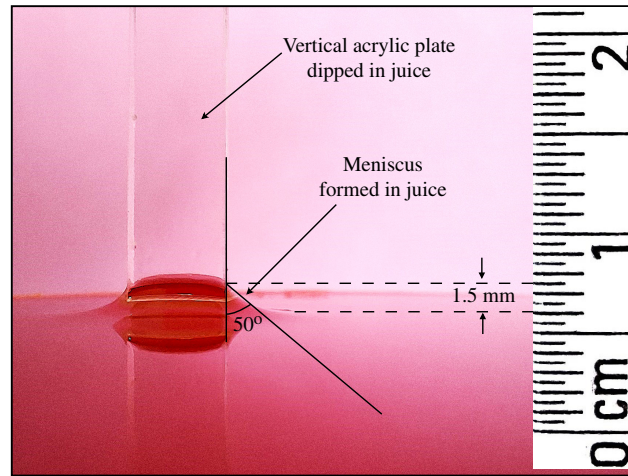


FIGURE 3. Determination of the dimensional parameters of the meniscus of watermelon juice on a vertical acrylic plate.

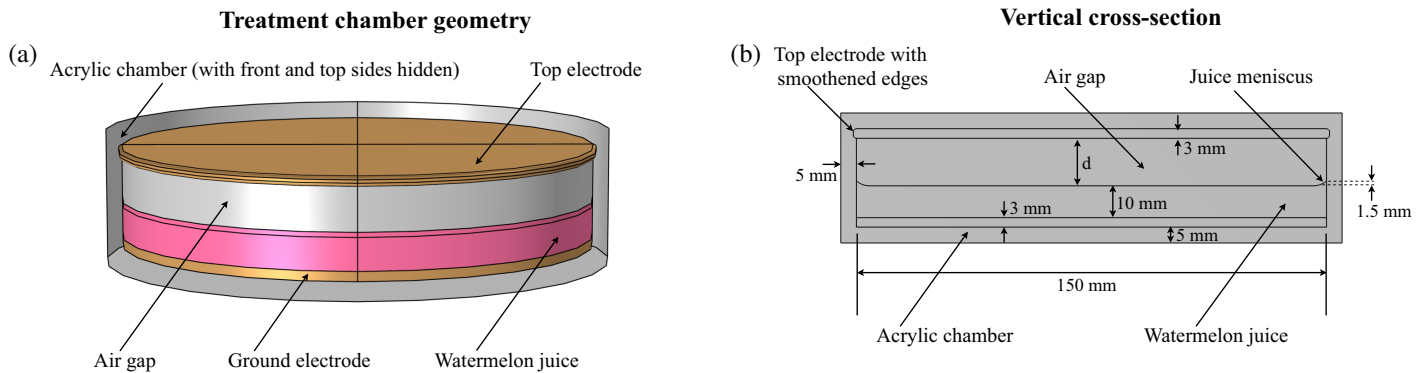


FIGURE 4. Geometry of the chamber used for simulation.

$$\mathbf{q} = -k\nabla T \quad (12)$$

where  $\rho$  is the density of the medium;  $C_p$  is the specific heat capacity at constant pressure;  $T$  is the absolute temperature;  $\mathbf{u}$  is the velocity vector;  $\nabla$  is the vector differential operator;  $\mathbf{q}$  is the heat flux by conduction;  $Q_{ted}$  is the thermoelastic damping;  $Q$  is the additional heat sources, such as Joule heating; and  $k$  is the thermal conductivity. According to Timmermans et al. [29], Eq. (13) can be used to calculate the energy density per pulse  $U$  from the electric field intensity  $\mathbf{E}$ , conductivity of the medium  $\sigma$ , and treatment duration  $\tau$ .

$$U = \mathbf{E}^2 \cdot \sigma \cdot \tau \quad (13)$$

$U$  gives the energy per unit volume per pulse for treatment with square pulses, where  $\mathbf{E}$  is constant. So, for treatment with double exponential pulses with varying values of  $\mathbf{E}$ , the specific energy input per pulse can be calculated by taking the volume integral of the product  $(\mathbf{E}^2 \cdot \sigma)$  and integrating it over the entire pulse duration. So, the specific energy input to the juice of mass  $m$  for  $n$  double exponential pulses is calculated using Eq. (14), and the values are mentioned in Section 3.2.6.

$$\text{Specific energy input} = \frac{n}{m} \int_{\text{pulse width}} \iiint_V (\mathbf{E}^2 \cdot \sigma) dt \quad (14)$$

The meniscus of the juice along the chamber wall affects the height of the air gap and intensifies the electric field. So it

was also included in the chamber geometry. To measure the dimensions of the meniscus, a vertical acrylic plate was dipped in watermelon juice (Fig. 3). The contact angle of the meniscus was measured as described by Medina et al. [30]. To measure the height of the meniscus, a photograph of a ruler taken from the same distance was superimposed on the picture as shown in Fig. 3.

The geometry consists of a hollow cylindrical chamber with an inner diameter of 150 mm, as shown in Fig. 4. The chamber wall, 5 mm thick, was made of Polymethyl Methacrylate (PMMA), with a heat capacity of 1420 J/(kg.K), relative permittivity of 3.0, density of 1190 kg/m<sup>3</sup>, and thermal conductivity of 0.19 W/(m.K). The electrical conductivity of PMMA is 10<sup>-14</sup> S/m [31]; the heat transfer coefficient is 10 W/(m<sup>2</sup>.K); and the surface emissivity is 0.96 [32].

The watermelon juice inside the cylinder was 10 mm in depth. The material properties assigned were electrical conductivity of 0.23 S/m, relative permittivity of 95 [27], density of 1033 kg/m<sup>3</sup> [33], heat capacity of 4050 J/(kg.K), and thermal conductivity of 0.616 W/(m.K) [34]. The space above the juice was filled with air with an electrical conductivity of 7.09 × 10<sup>-14</sup> S/m [35] and a relative permittivity of 1. The air surrounding the treatment chamber is represented by a large block of air, which is hidden in Fig. 4. The electrodes were made of UNS C26000 brass, 3 mm thick. The top electrode

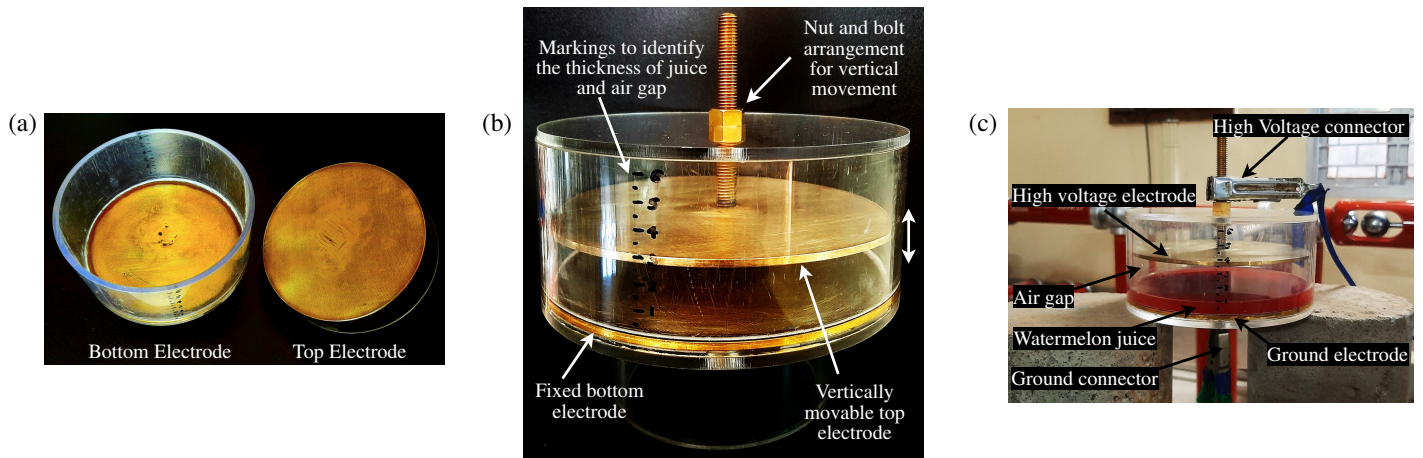


**FIGURE 5.** The chamber fabricated for PEF treatment. (a) Chamber in opened state. (b) Chamber in closed state. (c) PEF treatment using the chamber.

edges were rounded off (smoothing radius of 1 mm) to reduce the electric field intensity at the edges. The ambient temperature of the system was set to 298.15 K. The temperature increase after applying the double exponential pulse was simulated for different air gaps ( $d = 1.0$  cm to 4.5 cm), and the results are discussed in Section 3.1.1.

### 2.2.2. Simulation of Optimum Air Gap

To prevent electrical breakdown inside the chamber, the threshold height of the air gap for breakdown is required. Although the breakdown phenomenon depends on various factors, such as the electric field intensity, pressure, temperature, and electrode shape, it can be approximately predicted using the electric field intensity. The *Electrostatics* module in COMSOL was used for the simulation. The chamber geometry and material properties were the same as those described in Section 2.2.1. The electric field distribution inside the chamber for different values of air gap  $d$  was simulated to identify the threshold air gap that caused the breakdown, and the results are discussed in Section 3.1.3.

## 2.3. Experimental Assessment of Microbial Inactivation

Microbiological experiments were conducted to verify the effectiveness of the proposed method in inactivating microorganisms.

### 2.3.1. PEF Treatment Chamber

A parallel plate chamber was fabricated, as shown in Fig. 5, to perform the PEF treatment of watermelon juice. A parallel plate design was selected because it produces a uniform electric field distribution [36–38]. The chamber was made of acrylic, and brass electrodes were used. The bottom electrode is fixed. By adjusting the nut on the top connector rod, the top electrode can be moved vertically, allowing the air gap to be varied. The edges of the electrodes were rounded off to minimize the corner effect in the electric field.

### 2.3.2. Preparation of Juice

Watermelons (*Arka Manik* variety) were peeled; seeds were removed; and the juice was extracted by grinding the flesh for 3 minutes. Pulp was removed by filtering the juice through a 0.25-mm stainless steel sieve. *E. coli* was inoculated in 5 ml of freshly prepared and autoclaved nutrient broth and incubated overnight in a shaking incubator at 37°C. 1.25 ml of the overnight culture was used to inoculate 250 ml of sterilised watermelon juice for PEF treatment.

### 2.3.3. Experiment Procedure

The treatment chamber was filled to a height of 10 mm using inoculated juice. Double exponential pulses with the specifications mentioned in Section 2.1.1 were applied to the treatment chamber at a rate of 1 pulse per second using a modular AC/DC/impulse generator (W.S. Test Systems, Bangalore, India). Three treatment levels were used for each air gap, that is, 100, 200, and 300 pulses. Experiments were conducted in triplicates for each treatment level. Juice samples were collected in sterile Eppendorf tubes before and after treatment and kept on ice for microbial testing.

### 2.3.4. Microbiological Analysis

The collected samples were serially diluted using sterile distilled water to obtain  $10^{-1}$ ,  $10^{-2}$ ,  $10^{-3}$ , and  $10^{-4}$  dilutions. Then, 100  $\mu$ L of each diluted sample (inoculum) was spread on nutrient agar plates and incubated at 37°C. The number of colonies on each plate was counted after 24 hours. Only plates with colony counts between 20 and 300 were considered for calculating colony-forming units (CFU/mL) using Eq. (15), and the results are discussed in Section 3.2.2.

$$\text{Number of CFU/mL} = \text{Number of colonies} \times \frac{\text{Dilution factor}}{\text{Volume of sample taken (in mL)}} \quad (15)$$

### 2.3.5. Statistical Analysis

To evaluate the effect of the treatment parameters on microbial inactivation, a two-way Analysis of Variance (ANOVA) test was performed at a 99% confidence level ( $P < 0.01$ ). The air gap and number of pulses were considered as independent factors, whereas microbial inactivation was the dependent variable. Tukey's multiple comparison test was used for further analyses. Both analyses were conducted using OriginPro software (OriginLab Corporation).

The survival curves obtained for different treatment levels were fitted to a Weibull model [13] given by:

$$\log_{10} \frac{N}{N_0} = - \left[ \frac{n}{\delta} \right]^p \quad (16)$$

where  $N$  is the number of microbes (in CFU/mL) that had survived the treatment;  $N_0$  is the initial number of the microbial population;  $n$  is the number of pulses applied;  $p$  is the shape parameter; and  $\delta$  is the scale parameter of the curve. The estimated scale and shape parameters were determined using non-linear regression in origin. Based on the fitted model, the number of pulses required to achieve a 5-log reduction was also calculated. The results of the statistical analysis are discussed in Section 3.2.3.

### 2.3.6. Role of Dissolved Ions in Microbial Inactivation

Once microbial inactivation was achieved for a particular air gap, it was necessary to determine whether it was caused by the electric field or dissolved gas ions in the juice. Partial or full electrical breakdown in air can result in the creation of negative air ions [39]. Furthermore, if the juice is exposed to the high energies associated with the breakdown, it can dissociate water molecules in the juice into hydrogen and hydroxide ions [40]. The ability of negative air and hydroxide ions to inactivate microorganisms has already been reported [41–43]. Hence, it was necessary to check whether negative air and hydrogen ions were introduced into the juice during treatment.

The introduction of ions into a fluid can increase its conductivity [44, 45]. Therefore, if any gas ions were introduced into the juice owing to electrical breakdown during the treatment, the conductivity of the juice would increase. Additionally, the introduction of hydroxide and hydrogen ions can change the pH of the juice. Hence, the conductivity and pH values of the juice were measured before and immediately after PEF treatment. The conductivity was measured using a Conductivity Meter 304 (Systronics, Ahmedabad, India), and the pH was measured using a  $\mu$  pH System 361 (Systronics, Ahmedabad, India). The results of these measurements are discussed in Section 3.2.5.

## 3. RESULTS AND DISCUSSION

### 3.1. Simulation Results

Simulations were conducted for different air gaps (10, 15, 20, 25, 35, and 45 mm) using COMSOL Multiphysics software. In the following sections, only the sample results for certain air gaps are presented.

#### 3.1.1. Simulation of Power Dissipation and Temperature

A sample power dissipation density (loss density) surface plot at a vertical cross-section passing through the middle of the chamber, for an air gap of 2 cm at  $t = 0.25 \mu\text{s}$ , is shown in Fig. 6.

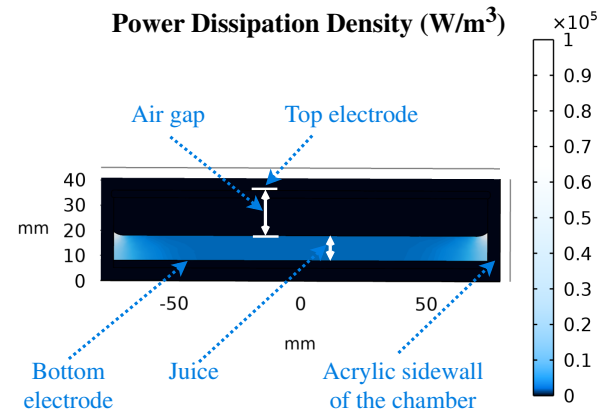


**FIGURE 6.** Surface plot of the power dissipation density obtained through simulation. Plots were prepared for various air gaps ranging from 1.0 cm to 4.5 cm. As a sample plot, the distribution for an air gap of 2 cm is shown.

Power dissipation was higher towards the edges of the juice, where the electric field was more intense owing to the corner effect. In addition, power dissipation decreased as the air gap increased. When analyzed over time, it was observed that the loss was considerably greater during the initial regions of the pulse, where the current waveform exhibited a spike, as shown in Fig. 2 (with an air gap). Then, volume plots of the juice temperature before and after applying the pulse were generated, with the ambient temperature set at 298.15 K. A comparison of the plots indicates that there is only a negligible increase in the juice temperature after applying one pulse. A sample temperature plot with a 2 cm air gap is shown in Fig. 7. The simulation results indicated that treatment with hundreds of pulses did not cause any measurable increase in juice temperature.

#### 3.1.2. Electric Field Distribution

The uniformity of the electric field distribution inside the chamber was analyzed with the help of contour plots. Filled contour plots were drawn for different air gaps ranging from 1.0 cm to 4.5 cm, as shown in Fig. 8. The figure displays only the electric field distribution within the juice. The contour plots show that the electric field is uniformly distributed throughout most of the juice, with minor variations confined to small regions near the juice meniscus and electrode edges. Maintaining this uniform electric field is essential to preventing inconsistent microbial inactivation within the chamber. The results also show that the electric field intensity increases as the air gap is reduced. So, lower air gaps can produce higher microbial inactivation.

The electric field distribution inside the chamber for different air gaps was analyzed to identify any potential chances of electrical breakdown. A sample volume plot of the electric field intensity inside the chamber for an air gap of 1.5 cm is shown in Fig. 9. The inset shows the surface plot of a selected portion of the vertical cross-section. Higher values of the electric field

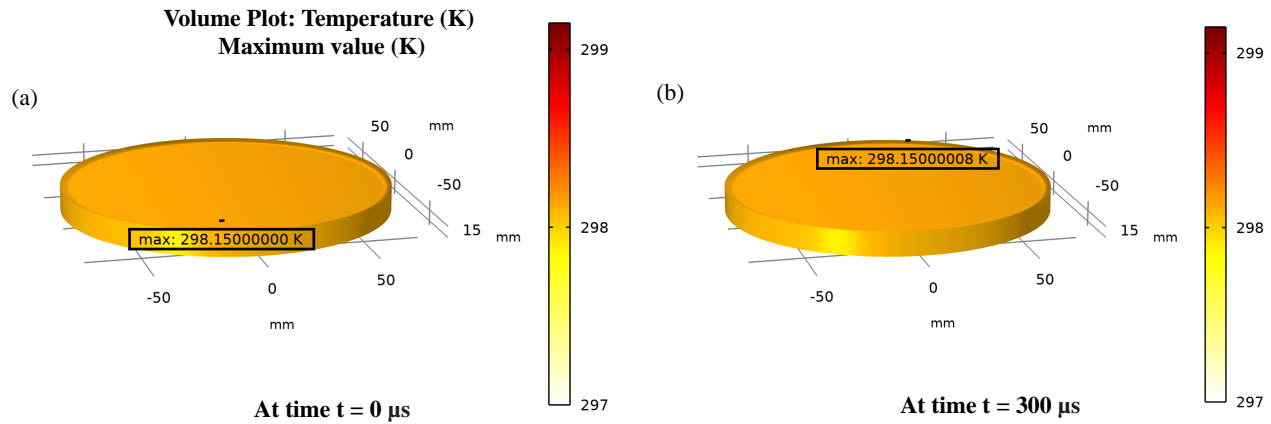


**FIGURE 7.** Volume plot of the temperature (along with the maximum value) inside the juice. Plots were prepared for various air gaps ranging from 1.0 cm to 4.5 cm. As a sample plot, the distribution for an air gap of 2 cm is shown. The chamber and air gap sections are hidden in the figure. (a) Juice temperature before treatment (b) Juice temperature after one pulse is applied.

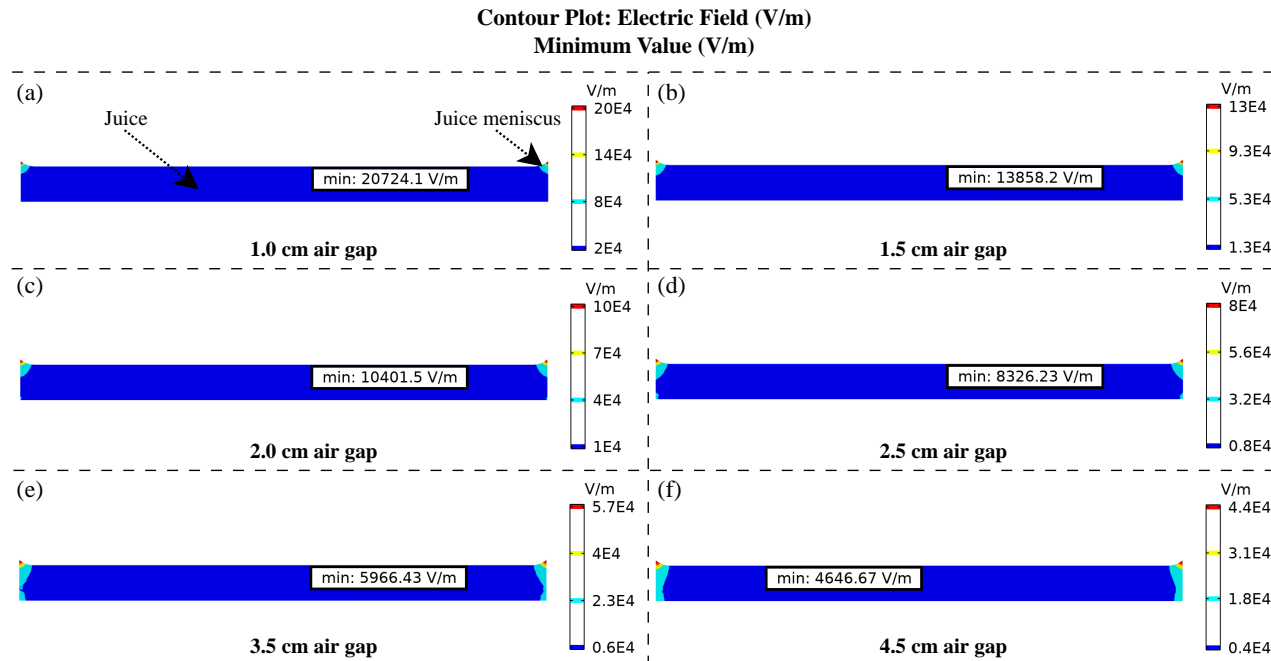


**FIGURE 8.** Filled contour plots of the normalized electric field intensity inside juice for different air gaps. The minimum value of electric field intensity is also shown. The chamber and air gap sections are hidden in the figure.

were observed near the edges of the electrodes and juice meniscus edge. If the electric field intensity in these regions exceeds the minimum threshold value for initiating the breakdown in air, it could lead to a breakdown in the air gap. Therefore, further analysis was conducted to determine the minimum air gap that could be provided without causing breakdown.

### 3.1.3. Optimum Air Gap through Simulation

The optimum value of the air gap is the one that produces the maximum power dissipation for microbial inactivation while preventing an electrical breakdown. Because the current signal was an impulse, the power dissipation at the instant that the current reached its peak was high. The peak values of the power dissipation density (power dissipation per unit volume

of juice) for various air gap values are shown in Fig. 10. As expected, the peak power dissipation density increased exponentially when the air gap was reduced. At lower air gap values, the peak power dissipation density exceeded  $1000 \text{ W/m}^3$ . Hence, from the simulation results, it was deduced that smaller air gaps were more effective in inactivating the microorganisms.

To check whether these smaller air gaps trigger electrical breakdown, electric field intensity plots, similar to those shown in Fig. 9, were analyzed. An imaginary outline was drawn by joining the points of the maximum electric field intensity, as shown in Fig. 11. In the volume and surface plots of the electric field intensity, points near the edge of the top electrode and the juice meniscus were observed to have the highest values of electric field inside the chamber. Therefore, a cutline was drawn to connect these points, ensuring that it contained the points with

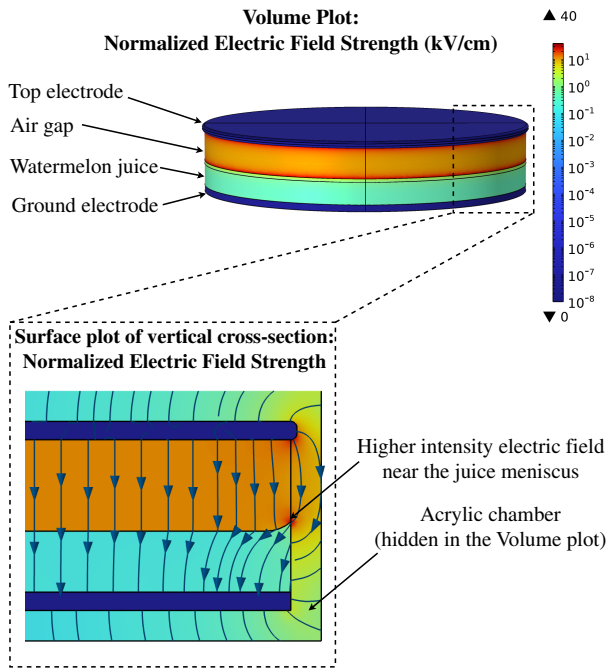


**FIGURE 9.** Normalized electric field intensity inside the chamber. Plots were prepared for various air gaps ranging from 1.0 cm to 4.5 cm. As a sample plot, the distribution for an air gap of 1.5 cm is shown.

the maximum values of field intensity in the air gap. The electric field intensity plots along this cutline for different air gaps are shown in Fig. 11.

The zero point on the  $x$ -axis in all plots corresponds to the edge of the top electrode, and the opposite end corresponds to the juice meniscus. The minimum value of the electric field strength required to initiate electrical breakdown in air is 30 kV/cm [46], and line L1 denotes that level. For a curve, if the electric field strength at any point is above the level L1, then it could initiate electrical breakdown. Also, the minimum field strength required for sustained propagation of the breakdown in air is 4.7 kV/cm [47], and line L2 denotes that level. For a particular curve, if the electric field strength at all points is above L2, then an initiated breakdown can be sustained. Plots for air gaps of 1.0 cm and 1.5 cm indicated a higher chance of electrical breakdown, as the field intensity near the juice meniscus exceeded L1. Therefore, a minimum air gap of 2.0 cm is required inside the chamber to prevent electrical breakdown. Hence, from the simulations, the optimal air gap inside the chamber was identified to be 2.0 cm. This method of estimating the air gap for electrical breakdown based on electric field values alone has its limitations. For greater accuracy, additional factors such as temperature, pressure, and other conditions also need to be taken into account. Therefore, the simulation results were later validated through experiments for a more comprehensive conclusion.

## 3.2. Experimental Validation of Simulation Results

### 3.2.1. Validation of Optimum Air Gap

During the experiments, the watermelon juice inside the chamber with different air gaps was treated with double exponential

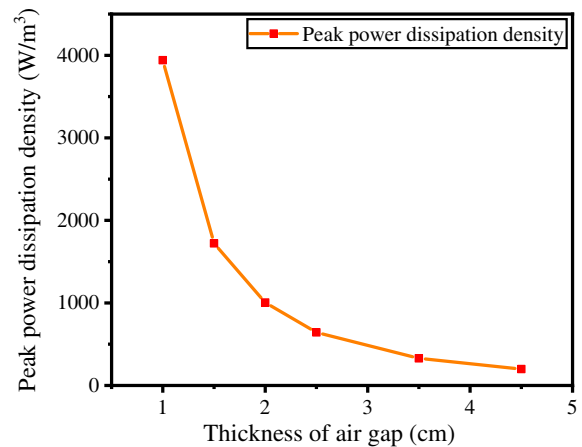


**FIGURE 10.** Peak values of power dissipation density for different air gaps. The power dissipation density values were obtained through simulations.

pulses with an amplitude of 20 kV. The applied voltage waveform captured using a Tektronix DPO 5104B Digital Phosphor Oscilloscope is shown in Fig. 12(a). The displayed image shows the voltage waveform after the attenuation in the ratio of 425 : 1, with the maximum voltage of the applied pulse reaching 20.825 kV. For each air gap, 20 pulses were applied at a rate of one pulse per second, and the number of visible breakdowns in the air gap was counted. For certain air gaps, electrical breakdowns occurred in the air gap associated with a cracking sound and bright light, as shown in Fig. 12(c). As expected, breakdowns occurred near the chamber sidewall, where the field intensity was higher.

The results of the experiments conducted in triplicate are shown in Fig. 13. Breakdowns occurred across the air gap when it was kept at 1.0 cm and 1.5 cm. Breakdown was not observed for air gaps of 2.0 cm or higher. These results match those obtained from the simulations. Hence, it was determined that a minimum air gap of 2 cm was required inside the chamber for PEF treatment of watermelon juice using double exponential pulses with an amplitude of 20 kV.

### 3.2.2. Microbial Inactivation Results

Microbiological experiments were conducted to verify the level of microbial inactivation in juice. Because air gaps below 2 cm were found to cause electrical breakdown, only air gaps of 2 cm, 2.5 cm, 3.5 cm, and 4.5 cm were considered for microbiological experiments. Microbial inactivation was measured using the procedure described in Section 2.3. The set of sample results obtained for an air gap of 2 cm with a  $10^{-2}$  dilution is shown in Fig. 14.

Figure 14 illustrates that the PEF treatment caused some level of microbial inactivation. For the actual calculation of CFU/mL as per Eq. (15), only plates with 20–300 colonies were used. The mean value of microbial concentration in the untreated sample was obtained as  $1.65 \times 10^6$  CFU/mL from triplicate measurements. The plot of  $\log(\text{CFU/mL})$  vs. the level of PEF treatment is shown in Fig. 15.

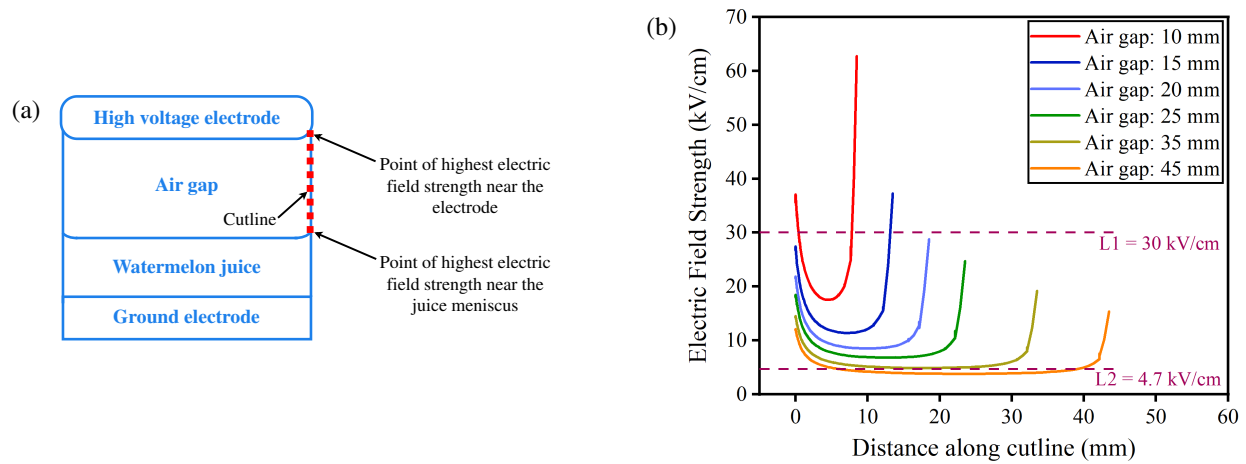


**FIGURE 11.** (a) Illustrative diagram of the imaginary cutline used to analyze the peak values of electric field strength within the air gap. (b) Plot of electric field strength along the cutline. Plots for various air gaps ranging from 10 mm to 45 mm are shown.

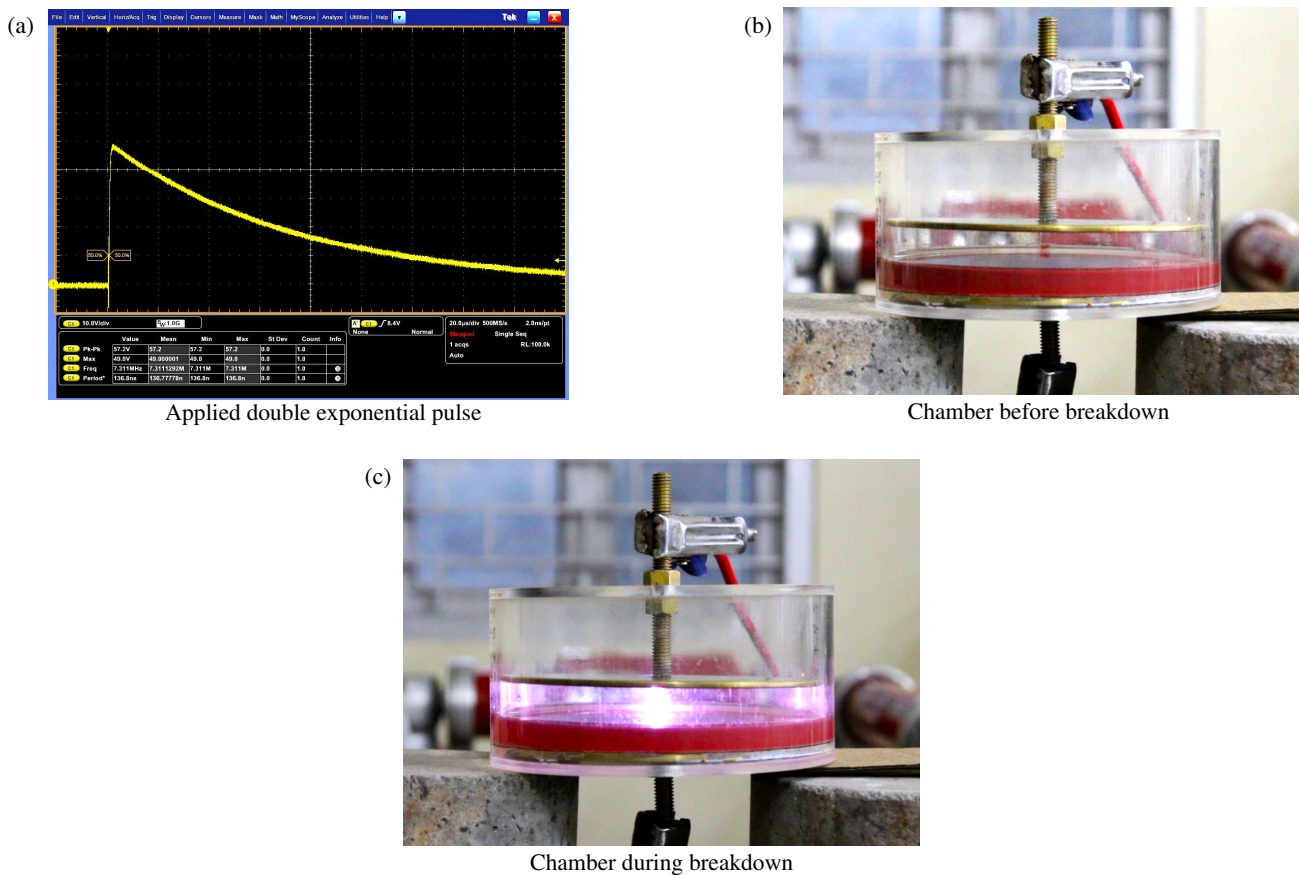


**FIGURE 12.** Electrical breakdown experiments conducted for various air gaps ranging from 1.0 cm to 4.5 cm. Sample images of the experiment with 1.5 cm air gap are shown. (a) Applied pulse captured using an oscilloscope after an attenuation in the ratio 425:1 (b) Chamber with an air gap of 1.5 cm, before applying the pulse (c) Chamber at the time of electrical breakdown of air.

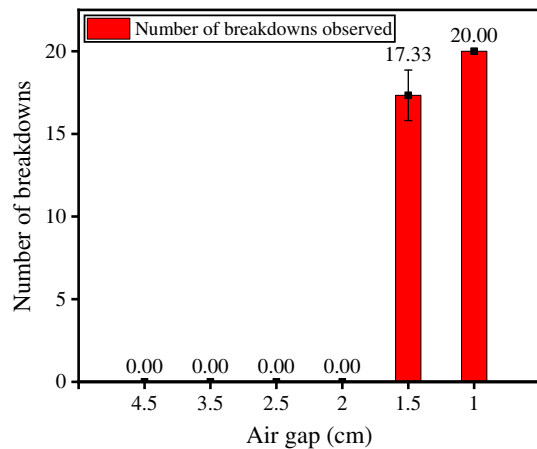
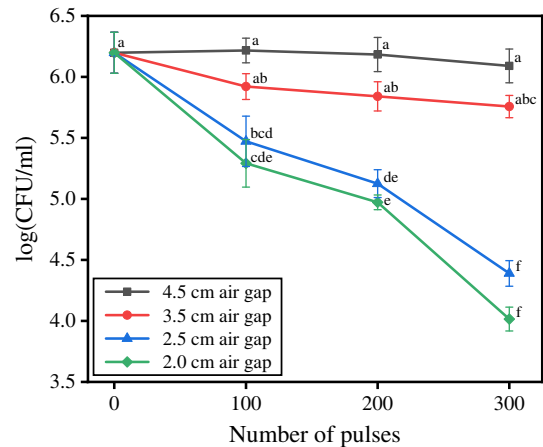
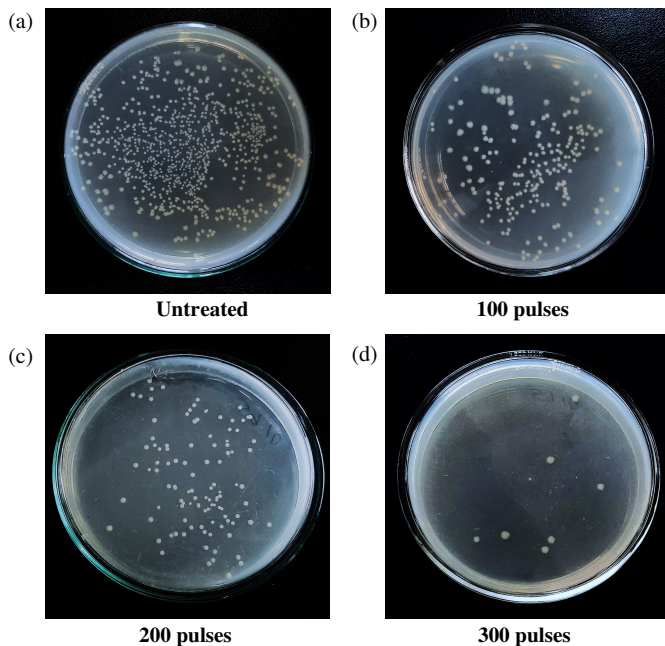
For a particular treatment level, the number of microbial colonies decreased as the air gap decreased. Additionally, for a specific air gap value, the number of colonies decreased with an increase in the number of pulses. This was because the reduced air gap and increased number of pulses resulted in greater power dissipation in the juice. Thus, inferences made from the simulations were experimentally validated.

### 3.2.3. Statistical Analysis of Experiment Results

ANOVA test results indicated a significant difference ( $P < 0.0001$ ) in microbial inactivation levels when the number of pulses varied. Variation in air gaps also resulted in significantly different inactivation levels (obtained P value  $< 0.0001$ ). Tukey's multiple comparison test was performed for further

**TABLE 1.** Temperature readings before and after the PEF treatment for various air gaps.

Air gap (cm)	Initial temperature (°C)	Temperature after 300 pulses (°C)
4.5	28.1	28.1
3.5	28.6	28.6
2.5	27.2	27.2
2	27.8	27.8

**FIGURE 13.** Number of electrical breakdowns observed inside the chamber during the experiment. Values are shown as mean  $\pm$  SD of readings in triplicate.**FIGURE 15.** Plot of log(CFU/mL) vs. number of pulses. Values are shown as mean  $\pm$  SD of measurements in triplicate. Values with different letters a-f are significantly different ( $P < 0.01$ ) based on the Tukey test.**FIGURE 14.** Spread-plated samples used during microbiological experiment. Microbiological experiments were conducted for various air gaps ranging from 2.0 cm to 4.5 cm. Only the plates for 2 cm air gap with a  $10^{-2}$  dilution are shown in the figure.

analysis. The results of the Tukey test are indicated using letters a–f in Fig. 15. It was observed that the PEF treatment with air gaps of 4.5 cm and 3.5 cm had no significant effect on the microbial count, even when 300 pulses were applied. How-

ever, air gaps of 2.5 cm and lower seemed to have a significant effect on the inactivation levels. The PEF treatment at 2.0 cm with 300 pulses resulted in the most significant reduction in the microbial counts (log(CFU/mL) reduced by 2.18 from the initial value) compared to all other treatment conditions and hence was the most effective among the considered treatment conditions.

The treatment parameters required to achieve an acceptable 5-log microbial reduction were estimated with the Weibull model using Eq. (16). For the treatment with a 2 cm air gap, it was estimated that a 5-log reduction can be achieved with 770 pulses.

### 3.2.4. Experimental Validation of Temperature Rise

The simulation results in Section 3.1.1 indicated that, in the absence of electrical breakdown, the temperature of the juice would not have any measurable increase. To validate these findings, the temperature of the juice was measured using a digital thermometer with a resolution of  $0.1^{\circ}\text{C}$ . For each air gap, readings were taken before applying any pulses and after applying 300 pulses, as shown in Table 1. Since air gaps of 1.0 cm and 1.5 cm were not considered for microbiological analysis due to the electrical breakdown, temperature readings were not taken for these cases. The results indicated that even after applying 300 pulses, there was no increase in temperature, as predicted by the simulation results. This also confirmed that there was no uncontrolled discharge of current into the juice, which could have caused microbial inactivation.

**TABLE 2.** Conductivity and pH readings of watermelon juice before and after the PEF treatment with a 2.0 cm air gap.

Processing stage	Conductivity (S/m)	pH
Before PEF treatment	0.29	5.39
After treatment with 300 pulses	0.29	5.39

**TABLE 3.** Comparison table of microbial reduction levels and specific energy inputs for PEF-based studies.

Reference	Microorganism	Log reduction	Treated medium	PEF treatment method	Specific energy input
Kantala et al. [4]	<i>E. coli</i>	5.95	Thai Orange Juice	Direct contact	66.7 kJ/L
Timmermans et al. [48]	<i>E. coli</i>	5.0	Apple juice	Direct contact	67 kJ/kg
Narsetti et al. [9]	<i>E. coli</i>	4.0	Water	Direct contact	40 kJ/L
Toepfl et al. [49]	<i>E. coli</i>	3.3	Ringer solution	Direct contact	80 kJ/kg
Timmermans et al. [20]	<i>E. coli</i>	2.0	Orange juice	Direct contact	25 kJ/kg
Novac et al. [6]	<i>E. coli</i>	6.0	Water	Ceramic coated electrodes	0.1 kJ/L
This work	<i>E. coli</i>	2.18	Watermelon juice	Chamber with an air gap	0.5 kJ/kg

### 3.2.5. Results of Conductivity and pH Measurements

From Section 3.2.2, it was observed that microbial inactivation was achieved with an air gap of 2.0 cm without any visible electrical breakdown. However, it was essential to verify that microbial inactivation was not due to negative air ions or hydroxide ions generated by partial breakdown. As explained in Section 2.3.6, the conductivity and pH of the juice were measured before and immediately after PEF treatment with a 2.0 cm air gap, and the results are presented in Table 2. Even after treatment with 300 pulses, no change was observed in the conductivity or pH of the juice. These results indicate that no dissolved ions were introduced into the juice as a result of PEF treatment.

### 3.2.6. Discussion on Inactivation Mechanisms

This study achieved microbial inactivation using electromagnetic fields without any noticeable increase in juice temperature. Previous studies on PEF treatment have reported similar or higher inactivation levels, but they have been achieved with an associated rise in temperature [4, 13]. This temperature rise was due to the high amount of specific energy (in the order of kJ/kg) that was input to the juice through the electric pulses. In this study, because the current pulses used were sharp impulses without any flat portions, the energy dissipated was significantly reduced, resulting in a negligible temperature rise. Because the conductivity and pH readings remained the same even after the PEF treatment, it could be concluded that microbial inactivation was not triggered by any partial electrical breakdown during the PEF treatment.

The main reasons for microbial inactivation in this study were the peak power dissipation density of the impulse signals and the increased number of pulses. As discussed in Section 3.1.3, the value of the power dissipation density at the peak of the applied impulse signal was high. Additionally, the number of pulses applied in this work was much higher than that in previous studies. Therefore, repeated application of these pulses with a high power density triggered electroporation in microbial organisms. Even though the electric field strength

was lower across the juice than across the air gap, the application of these pulses in large numbers contributed to the lethal effect.

To compare the results of this study with previous studies, the specific energy input has been calculated from simulated electric field intensities using Eq. (14). Table 3 compares this study with various studies that used PEF treatment for the inactivation of *E. coli*. It is observed that the log reductions reported in various studies differ significantly. This variation arises because key processing parameters, such as electric field intensity, type of treated medium, pulse width, treatment duration, and chamber configuration, vary widely across studies. Studies with high specific energy inputs have used a direct-contact treatment method, in which both electrodes were in direct contact with the treated medium. Hence, high current flow and associated Joule heating were present in those cases. The energy requirements for chambers without direct contact are much lower. Novac et al. [6] obtained a 6-log reduction with only 0.1 kJ/L using electrodes coated with ceramic that prevented the Joule heating. However, the inactivation was achieved with a very high electric field of 200 kV/cm. In contrast, the present study employed a lower electric field strength, which justifies the lower level of microbial inactivation.

In this study, a 2-log microbial reduction was achieved using 300 pulses. According to the results of the Weibull model estimation in Section 3.2.3, applying 770 pulses can achieve a 5-log reduction, which is a commonly accepted level of inactivation. Microbial inactivation can also be increased by re-designing the chamber to accommodate a thinner air gap without causing electrical breakdown. Further research on this treatment method could lead to higher levels of microbial inactivation with lower current consumption compared with previous studies.

## 4. CONCLUSIONS

A method to reduce the current requirement during PEF treatment by introducing an air gap inside the chamber was pro-

posed. Using a mathematical model, the current flow during the proposed treatment was proven to be much smaller than that reported in previous studies. Simulations using COMSOL Multiphysics software revealed that PEF treatment using the proposed system did not cause a noticeable increase in temperature. Simulations of the electric field distribution were used to determine the minimum air gap value that could be introduced into the chamber without causing electrical breakdown. The accuracy of this result was verified by performing PEF experiments with a fabricated chamber. Both the simulation and experimental results indicated that PEF treatment with 20 kV pulses could be performed without electrical breakdown if a minimum air gap of 2 cm was maintained inside the chamber. The effectiveness of the proposed system for microbial inactivation was assessed through microbiological experiments with varying air gaps. High-voltage pulses were applied to watermelon juice inoculated with *E. coli* and the extent of microbial reduction was measured after different levels of PEF treatment. In the experiments, the application of 300 double exponential pulses to the chamber with a 2 cm air gap resulted in a 2-log reduction in microorganisms. Higher levels of microbial inactivation can be achieved by applying more pulses or modifying the chamber design to accommodate thinner air gaps without electrical breakdown. Thus, the proposed system of treatment chambers containing air gaps can be used for future PEF treatments with pulse generators having low ampere ratings.

## ACKNOWLEDGEMENT

The author(s) acknowledge that access to COMSOL Multiphysics software was provided by I-STEM (Indian Science Technology and Engineering facilities Map), supported by the Office of the Principal Scientific Adviser to the Government of India. The author(s) also acknowledge the Department of Chemistry, National Institute of Technology Calicut, for facilitating the measurement of the pH and conductivity.

## REFERENCES

- [1] Lee, H., S. Choi, E. Kim, Y.-N. Kim, J. Lee, and D.-U. Lee, "Effects of pulsed electric field and thermal treatments on microbial reduction, volatile composition, and sensory properties of orange juice, and their characterization by a principal component analysis," *Applied Sciences*, Vol. 11, No. 1, 186, 2021.
- [2] Rahaman, A., X.-A. Zeng, M. A. Farooq, A. Kumari, M. A. Murtaza, N. Ahmad, M. F. Manzoor, S. Hassan, Z. Ahmad, B.-R. Chen, J. Zhan, and A. Siddeeg, "Effect of pulsed electric fields processing on physiochemical properties and bioactive compounds of apricot juice," *Journal of Food Process Engineering*, Vol. 43, No. 8, e13449, 2020.
- [3] Dziadek, K., A. Kopeć, T. Drózdź, P. Kielbasa, M. Ostafin, K. Bulski, and M. Oziembłowski, "Effect of pulsed electric field treatment on shelf life and nutritional value of apple juice," *Journal of Food Science and Technology*, Vol. 56, No. 3, 1184–1191, 2019.
- [4] Kantala, C., S. Supasin, P. Intra, and P. Rattanadecho, "Evaluation of pulsed electric field and conventional thermal processing for microbial inactivation in thai orange juice," *Foods*, Vol. 11, No. 8, 1102, Apr. 2022.
- [5] Lopes, S. J. S., A. S. Sant'Ana, and L. Freire, "Non-thermal emerging processing technologies: Mitigation of microorganisms and mycotoxins, sensory and nutritional properties maintenance in clean label fruit juices," *Food Research International*, Vol. 168, 112727, Jun. 2023.
- [6] Novac, B. M., F. A. Banakhr, I. R. Smith, L. Pecastaing, R. Ruscassie, A. S. d. Ferron, and P. Pignolet, "Demonstration of a novel pulsed electric field technique generating neither conduction currents nor Joule effects," *IEEE Transactions on Plasma Science*, Vol. 42, No. 1, 216–228, Jan. 2014.
- [7] Brito, I. P. C. and E. K. Silva, "Pulsed electric field technology in vegetable and fruit juice processing: A review," *Food Research International*, Vol. 184, 114207, May 2024.
- [8] Krishnaveni, S., R. Subhashini, and V. Rajini, "Inactivation of bacteria suspended in water by using high frequency unipolar pulse voltage," *Journal of Food Process Engineering*, Vol. 40, No. 6, e12574, Dec. 2017.
- [9] Narsetti, R., R. D. Curry, K. F. McDonald, T. E. Clevenger, and L. M. Nichols, "Microbial inactivation in water using pulsed electric fields and magnetic pulse compressor technology," *IEEE Transactions on Plasma Science*, Vol. 34, No. 4, 1386–1393, Aug. 2006.
- [10] Qin, S., I. V. Timoshkin, M. Maclean, S. J. MacGregor, M. P. Wilson, M. J. Given, T. Wang, and J. G. Anderson, "TiO<sub>2</sub>-coated electrodes for pulsed electric field treatment of microorganisms," *IEEE Transactions on Plasma Science*, Vol. 44, No. 10, 2121–2128, Oct. 2016.
- [11] Mihindukulasuriya, S. D. F. and S. H. Jayaram, "Release of electrode materials and changes in organoleptic profiles during the processing of liquid foods using pulse electric field treatment," *IEEE Transactions on Industry Applications*, Vol. 56, No. 1, 711–717, Jan.–Feb. 2020.
- [12] Gad, A. and S. H. Jayaram, "Processing of carbonated beer by pulsed electric fields," *IEEE Transactions on Industry Applications*, Vol. 51, No. 6, 4759–4765, Nov.–Dec. 2015.
- [13] Delso, C., S. Ospina, A. Berzosa, J. Raso, and I. Álvarez Lanza, "Defining winery processing conditions for the decontamination of must and wine spoilage microbiota by Pulsed Electric Fields (PEF)," *Innovative Food Science & Emerging Technologies*, Vol. 89, 103478, Oct. 2023.
- [14] Zhang, R., N. Zheng, H. Liu, and L. Wang, "Influencing factors of dielectric breakdown in the pef treatment chamber," *IEEE Transactions on Plasma Science*, Vol. 43, No. 2, 610–616, Feb. 2015.
- [15] Zhao, P., C. Liao, W. Lin, and J. Feng, "Effects of microwave frequency on electron energy distribution function and air breakdown using the fluid model," *Progress In Electromagnetics Research M*, Vol. 26, 279–287, 2012.
- [16] Kumar, V., D. Kohli, B. Naik, A. Ratore, A. K. Gupta, J. M. Khan, M. Irfan, M. S. Preet, N. Chatterjee, and S. Rustagi, "Effect of heat treatment on the quality of citrus juices," *Journal of King Saud University-Science*, Vol. 35, No. 7, 102819, 2023.
- [17] Kannan, S., S. R. S. Dev, Y. Garipey, and V. G. S. Raghavan, "Effect of radiofrequency heating on the dielectric and physical properties of eggs," *Progress In Electromagnetics Research B*, Vol. 51, 201–220, 2013.
- [18] Wu, W. J. and J. Chang, "Inactivation of vegetative cells, germinated spores, and dormant spores of bacillus atrophaeus by pulsed electric field with fixed energy input," *Journal of Food Process Engineering*, Vol. 45, No. 2, e13959, 2022.
- [19] Zhong, K., F. Chen, J. Wu, Z. Wang, X. Liao, X. Hu, and Z. Zhang, "Kinetics of inactivation of escherichia coli in carrot juice by pulsed electric field," *Journal of Food Process Engineering*

- neering, Vol. 28, No. 6, 595–609, Dec. 2005.
- [20] Timmermans, R. A. H., H. C. Mastwijk, L. B. J. M. Berendsen, A. L. Nederhoff, A. M. Matser, M. A. J. S. V. Boekel, and M. N. N. Groot, “Moderate intensity Pulsed Electric Fields (PEF) as alternative mild preservation technology for fruit juice,” *International Journal of Food Microbiology*, Vol. 298, 63–73, Jun. 2019.
- [21] Bhattacharjee, C., V. K. Saxena, and S. Dutta, “Novel thermal and non-thermal processing of watermelon juice,” *Trends in Food Science & Technology*, Vol. 93, 234–243, Nov. 2019.
- [22] Ma, T., J. Wang, H. Wang, T. Lan, R. Liu, T. Gao, W. Yang, Y. Zhou, Q. Ge, Y. Fang, and X. Sun, “Is overnight fresh juice drinkable? the shelf life prediction of non-industrial fresh watermelon juice based on the nutritional quality, microbial safety quality, and sensory quality,” *Food & Nutrition Research*, Vol. 64, 10–29 219, 2020.
- [23] Pinto, C., S. A. Moreira, L. G. Fidalgo, M. D. Santos, I. Delgado, and J. A. Saraiva, “Shelf-life extension of watermelon juice preserved by hyperbaric storage at room temperature compared to refrigeration,” *LWT — Food Science and Technology*, Vol. 72, 78–80, 2016.
- [24] Wang, G., Y. Zhang, and Z. Qiao, “Temperature field simulation of submarine cable under different laying environments based on COMSOL,” *Progress In Electromagnetics Research C*, Vol. 154, 111–117, 2025.
- [25] Timoshkin, I. V., S. J. MacGregor, R. A. Fouracre, B. H. Crichton, and J. G. Anderson, “Transient electrical field across cellular membranes: Pulsed electric field treatment of microbial cells,” *Journal of Physics D: Applied Physics*, Vol. 39, No. 3, 596–603, 2006.
- [26] Magdowski, M. and R. Vick, “Estimation of the mathematical parameters of double-exponential pulses using the Nelder-Mead algorithm,” *IEEE Transactions on Electromagnetic Compatibility*, Vol. 52, No. 4, 1060–1062, Nov. 2010.
- [27] Guo, W., X. Zhu, and S. O. Nelson, “Permittivities of watermelon pulp and juice and correlation with quality indicators,” *International Journal of Food Properties*, Vol. 16, No. 3, 475–484, Jan. 2013.
- [28] Laissaoui, A., A. Abdi, S. Mezoued, B. Nekhoul, and D. Poljak, “Transient thermal analysis of human exposure to electromagnetic fields,” *Progress In Electromagnetics Research M*, Vol. 112, 93–104, 2022.
- [29] Timmermans, R. A. H., A. L. Nederhoff, M. N. N. Groot, M. A. J. S. V. Boekel, and H. C. Mastwijk, “Effect of electrical field strength applied by PEF processing and storage temperature on the outgrowth of yeasts and moulds naturally present in a fresh fruit smoothie,” *International Journal of Food Microbiology*, Vol. 230, 21–30, 2016.
- [30] Medina, A., A. López-Villa, and C. A. Vargas, “Functional acrylic surfaces obtained by scratching,” *Fluids*, Vol. 6, No. 12, 463, Dec. 2021.
- [31] Zheng, W. and S.-C. Wong, “Electrical conductivity and dielectric properties of PMMA/expanded graphite composites,” *Composites Science and Technology*, Vol. 63, No. 2, 225–235, Feb. 2003.
- [32] Jiang, F., J. L. de Ris, and M. M. Khan, “Absorption of thermal energy in PMMA by in-depth radiation,” *Fire Safety Journal*, Vol. 44, No. 1, 106–112, Jan. 2009.
- [33] Milczarek, R. R., C. W. Olsen, and I. Sedej, “Quality of watermelon juice concentrated by forward osmosis and conventional processes,” *Processes*, Vol. 8, No. 12, 1568, Nov. 2020.
- [34] Mukama, M., A. Ambaw, and U. L. Opara, “Thermophysical properties of fruit — a review with reference to postharvest handling,” *Journal of Food Measurement and Characterization*, Vol. 14, No. 5, 2917–2937, 2020.
- [35] Kumar, V. S., S. Sampath, S. M. Das, and K. V. Kumar, “Atmospheric electrical conductivity variations over different environments,” *Geophysical Journal International*, Vol. 122, No. 1, 89–96, Jul. 1995.
- [36] Masood, H., Y. Diao, P. J. Cullen, N. A. Lee, and F. J. Trujillo, “A comparative study on the performance of three treatment chamber designs for radio frequency electric field processing,” *Computers & Chemical Engineering*, Vol. 108, 206–216, Jan. 2018.
- [37] Mohan, T., K. J. Suja, and K. Sunitha, “a multi-electrode system for pulsed electric field treatment chamber,” *Journal of Food Engineering*, Vol. 371, 111995, Jun. 2024.
- [38] Chandanasree, G., T. Mohan, and K. J. Suja, “Modeling and analysis of pulsed electric field treatment chambers for liquid food processing,” in *Perspectives on Global Transformation*, Vol. 1368, 123–135, 2025.
- [39] Lin, H.-F. and J.-M. Lin, “Generation and determination of negative air ions,” *Journal of Analysis and Testing*, Vol. 1, No. 1, 6, 2017.
- [40] Clements, J. S., M. Sato, and R. H. Davis, “Preliminary investigation of prebreakdown phenomena and chemical reactions using a pulsed high-voltage discharge in water,” *IEEE Transactions on Industry Applications*, Vol. IA-23, No. 2, 224–235, Mar. 1987.
- [41] Rusdiana Puspa Dewi, S., R. A. Santoso, B. Sujatmiko, and I. S. Wibowo, “Antibacterial activity of various calcium hydroxide solvents against *Fusobacterium nucleatum* and *Enterococcus faecalis*,” in *Journal of Physics: Conference Series*, Vol. 1246, No. 1, 012010, 2019.
- [42] Noyce, J. O. and J. F. Hughes, “Bactericidal effects of negative and positive ions generated in nitrogen on *Escherichia coli*,” *Journal of Electrostatics*, Vol. 54, No. 2, 179–187, Feb. 2002.
- [43] Seo, K. H., B. W. Mitchell, P. S. Holt, and R. K. Gast, “Bactericidal effects of negative air ions on airborne and surface salmonella enteritidis from an artificially generated aerosol,” *Journal of Food Protection*, Vol. 64, No. 1, 113–116, Jan. 2001.
- [44] Light, T. S., S. Licht, A. C. Bevilacqua, and K. R. Morash, “The fundamental conductivity and resistivity of water,” *Electrochemical and Solid-State Letters*, Vol. 8, No. 1, E16–E19, 2005.
- [45] Pawlowicz, R., “Calculating the conductivity of natural waters,” *Limnology and Oceanography: Methods*, Vol. 6, No. 9, 489–501, Sep. 2008.
- [46] Lowke, J. J., “Theory of electrical breakdown in air—the role of metastable oxygen molecules,” *Journal of Physics D: Applied Physics*, Vol. 25, No. 2, 202–210, 1992.
- [47] Warne, L. K., R. E. Jorgenson, and E. E. Kunhardt, “Criterion for spark-breakdown in non-uniform fields,” *Journal of Applied Physics*, Vol. 115, No. 14, 143303, Apr. 2014.
- [48] Timmermans, R. A. H., M. N. N. Groot, A. L. Nederhoff, M. A. J. S. V. Boekel, A. M. Matser, and H. C. Mastwijk, “Pulsed electric field processing of different fruit juices: Impact of pH and temperature on inactivation of spoilage and pathogenic microorganisms,” *International Journal of Food Microbiology*, Vol. 173, 105–111, 2014.
- [49] Toepfl, S., V. Heinz, and D. Knorr, “High intensity pulsed electric fields applied for food preservation,” *Chemical Engineering and Processing: Process Intensification*, Vol. 46, No. 6, 537–546, 2007.